

USE OF A RIGOROUS MODEL IN THE CONTROL DESIGN OF A 3-D.O.F. HELICOPTER

ARTHUR CASTELLO BRANCO DE OLIVEIRA*, BRUNO AUGUSTO ANGÉLICO*

**Dept. de Engenharia de Telecomunicações e Controle
Escola Politécnica da USP
São Paulo, SP - Brasil*

Emails: `arthur.castello.oliveira@usp.br`, `angelico@lac.usp.br`

Abstract— In this paper it is studied the effect of using a linearized model based on a rigorous non-linear mechanical model on the design of a LQR control for a 3-d.o.f. Helicopter. It is presented a simpler model and one obtained with the Newton-Euler iterative algorithm. It is noticeable that the complete model, when linearized, shows a different structure than the simpler one, rather than just different parameters. This difference implies changes in the behavior of the model and results in better controllers for this system. To validate the superiority of the complete model it was applied both controllers on the real system and present the results.

Keywords— LQR, Newton-Euler Iterative Method, 3 DOF Helicopter

Resumo— Neste trabalho é estudado o efeito de usar um modelo linearizado baseado em um modelo mecânico não linear rigoroso no design de um controlador LQR para um helicóptero de bancada com três graus de liberdade. Apresenta-se um modelo mais simples e um obtido com o método iterativo de Newton-Euler. Nota-se que o modelo completo, quando linearizado, apresenta uma estrutura diferente do mais simples, ao invés de apenas diferentes parâmetros. Esta diferença implica em mudanças no comportamento do modelo e resulta em melhores controladores para este sistema. Para validar a superioridade do modelo completo, foram aplicados ambos controladores na planta real e apresentados os resultados.

Palavras-chave— LQR, Método Iterativo de Newton-Euler, Helicóptero de 3 graus de liberdade.

1 Introduction

The 3-dof helicopter is a plant frequently used in laboratories around the world and it is very non-linear and coupled besides being sub-actuated and unstable. This system presents a control challenge and the fact that it is available commercially motivates works with it.

In (Zheng and Zhong, 2011) and (Liu et al., 2013) the authors use the system to test robust designs based on LQR. Both solve the problem of robust attitude control for the 3-d.o.f. helicopter for the elevation and roll angle, but present no results for the travel angle.

In (Liu et al., 2014) the authors propose a hierarchical control of all three helicopter angles. This method consists in using the controlled pitch angle as an actuator for the travel angle. The paper uses the same control structure as the previous ones, but applied also on the travel and obtains great results for all angles.

In other works such as (Boby et al., 2014) and (Choudhary, 2014) the authors use LQR-derived controllers in the same system, but present only simulation results. In (Pereira and Kienitz, 2014) the author proposes a generalization of the LQG/LTR controller and obtains great practical results for all three angles as well.

In most of the works presented the authors use the Quanser system to test the control algorithms, which already has ready computer-system communication, a consolidated model and good sensors for all three angles.

In this work, a 3-d.o.f. system is built and a mathematical model is developed. The LQR is applied in two different models: one calculated using simplified models of each angle and the other one developed in this work using the Newton-Euler iterative method. The control algorithm was embedded in a LPC1768 microcontroller and the sensors were not as good as the ones at the Quanser system, which resulted in performance limitations.

2 Model and System Overview

This section revises the steps taken on the development of both models used on the paper, as well as studies the hardware limitations, such as encoders quantization and IMU noises.

The notations used during the modeling are presented below:

$\lambda(t)$	Travel Angle;
$\xi(t)$	Elevation Angle;
$p(t)$	Pitch Angle;
$\omega_f(t)$	Front motor rotation speed;
$\omega_b(t)$	Back motor rotation speed;
K_e	Force conversion constant;

It is considered that the relation between angular speed and generated force is perfectly quadratic in a helice-motor system, i.e.

$$F_{f,b} = K_e \cdot \omega_{f,b}^2$$

2.1 Simplified Linear Model

As can be seen in Figure 1, if it is assumed that the Center of Mass (CM) of the link is aligned with

its rotation axis, the pitch joint can be modeled as an inertial system with a binary as actuator and an inertia of J_p , as shown in Equation 1.

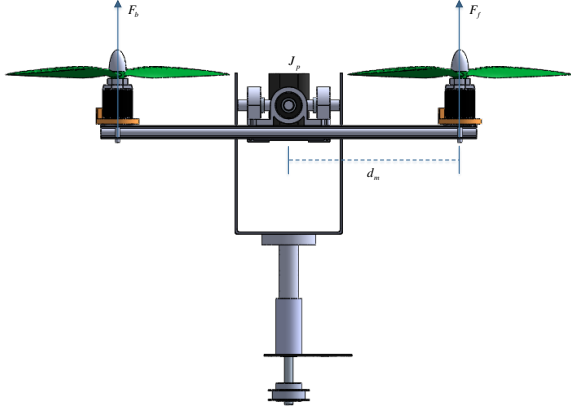


Figure 1: Pitch Angle Modeling

$$J_p \cdot \ddot{p} = K_e \cdot (\omega_f^2 - \omega_b^2) \cdot d_m \quad (1)$$

Considering this model, the pitch angle can be simplified as not being coupled and having quicker dynamics if compared with the other angles. Later in this paper it is shown that the assumption that the pitch CM is aligned with its rotation axis is not entirely correct for the system built, but this equation is the same presented in (Liu et al., 2013), (Zheng and Zhong, 2011) and (Boby et al., 2014). Therefore, this simplified model was considered here.

As for the elevation joint (Figure 2), since the CM is not aligned with its rotation axis, there is a constant gravity force that must be compensated in order for the horizontal to be a stability point. To deal with this issue, incremental variables were considered for the elevation angle.

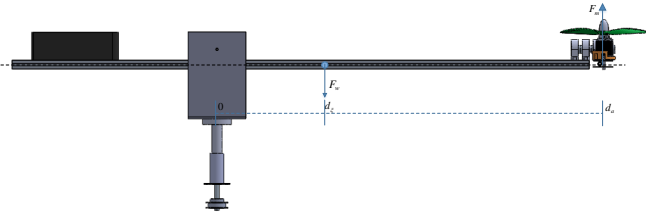


Figure 2: Elevation Angle Modeling

$$J_\xi \cdot \ddot{\xi} = -(m_\xi \cdot g \cdot d_\xi + m_p \cdot g \cdot d_a) \cdot \cos(\xi) + K_e \cdot (\omega_f^2 + \omega_b^2) \cdot d_a \cdot \cos(p)$$

Linearizing for small angles and assuming $\omega_f^2 + \omega_b^2 = \Omega_m$, with $\bar{\Omega}_m$ and $\hat{\Omega}_m$ as its fixed and varying part, respectively. Adjusting $\bar{\Omega}_m$ to compensate the gravity torque, results in:

$$\begin{aligned} J_\xi \cdot \ddot{\xi} &= -m_\xi \cdot g \cdot d_\xi - m_p \cdot g \cdot d_a \\ &+ K_e \cdot \bar{\Omega}_m \cdot d_a + K_e \cdot \hat{\Omega}_m \cdot d_a \rightarrow \\ &\rightarrow J_\xi \cdot \ddot{\xi} = K_e \cdot (\hat{\omega}_f^2 + \hat{\omega}_b^2) \cdot d_a \end{aligned} \quad (2)$$

Therefore, the elevation angle also behaves as an inertial system, considered the fact that it is necessary to add a constant value to the control signal. It is worth noting that, despite coupling in the non-linear simplified equation with the pitch angle, the final linearized model is uncoupled.

Finally, from Figure 3, it is noticeable that the travel angle is only actuated if the pitch angle is not null.

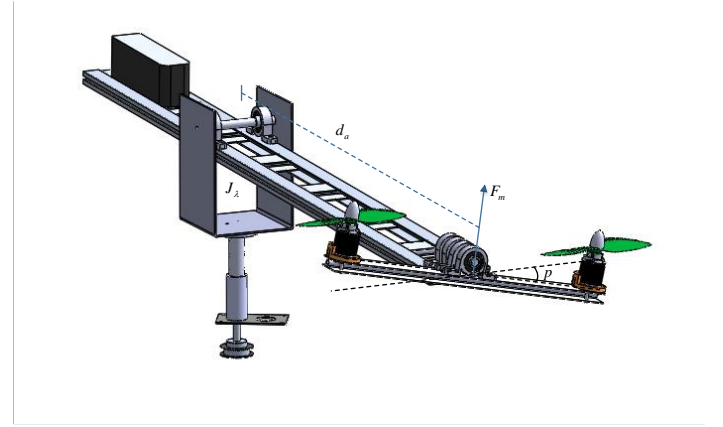


Figure 3: Travel Angle Modeling

$$J_\lambda \cdot \ddot{\lambda} = K_e \cdot \Omega_m \cdot d_a \cdot \sin(p)$$

Again, linearizing for small angles and applying the first order Taylor series for $p_0 = 0$ and $\Omega_{m0} = \bar{\Omega}_m$, results in:

$$J_\lambda \cdot \ddot{\lambda} = K_e \cdot \bar{\Omega}_m \cdot d_a \cdot p$$

It is worth noticing that the coupling appears on the linear model of the travel axis and that the control input have no effect on this state.

Finally, combining the equations in a state space model, equation 3 is obtained.

$$\begin{aligned}
A &= \begin{bmatrix} 0 & 0 & 0 & 1 & 0 & 0 \\ 0 & 0 & 0 & 0 & 1 & 0 \\ 0 & 0 & 0 & 0 & 0 & 1 \\ 0 & 0 & 0 & 0 & 0 & 0 \\ 0 & 0 & 0 & 0 & 0 & 0 \\ 0 & \frac{\bar{F}_m \cdot d_a}{J_\lambda} & 0 & 0 & 0 & 0 \end{bmatrix} \\
B &= \begin{bmatrix} 0 & 0 \\ 0 & 0 \\ 0 & 0 \\ \frac{K_e \cdot d_a}{J_\xi} & \frac{K_e \cdot d_a}{J_\xi} \\ \frac{K_e \cdot d_m}{J_p} & -\frac{K_e \cdot d_m}{J_p} \\ 0 & 0 \end{bmatrix} \\
x &= [\xi \quad p \quad \lambda \quad \dot{\xi} \quad \dot{p} \quad \dot{\lambda}]^T
\end{aligned} \tag{3}$$

Which is the exact same model presented by Quanser on the Maple document about the 3 d.o.f. helicopter modeling. This model is used in academic papers, such as (Choudhary, 2014).

2.2 Rigorous Nonlinear Model and Linearization

For modeling all nonlinear effects of this system, the iterative method of Newton-Euler was used, as described in (Craig, 2005), with the Denavit-Hartenberg parameters of Table 1.

Table 1: Parâmetros de D-H

j	α	a	θ	d
1	0	0	θ_1	0
2	$-\frac{\pi}{2}$	0	θ_2	0
3	$-\frac{\pi}{2}$	0	θ_3	L

All the joints torque are null and the inputs of the system are the forces and torques applied on the end of the manipulator — or in this case, the center of the pitch joint and moving with it — as can be seen in Figure 4.

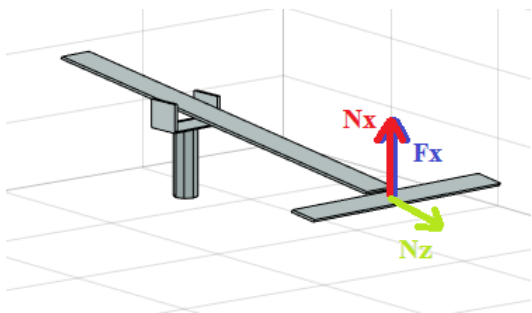


Figure 4: System Inputs

The two inputs directly caused by the controller are Fx and Nz . Nx is the drag torque of the helices and was included in the model for simulation purposes. It was not considered during control design mainly due to the fact that it is much smaller than the other inputs.

To estimate the mechanicals parameters of the model — since system identification is very difficult due to the fact that the system is unstable in open loop — a CAD model of the system was built. Other parameters (like motors time and speed-force constants) were estimated by system identification.

As mentioned before, from the CAD model it was observed that the CM of the pitch joint was slightly dislocated below its rotation axis and would behave more like a pendulum than an inertial system. Therefore, the displacement of the pitch CM, although small, was considered on this model.

The final model obtained is shown in equation (4).

$$\begin{aligned}
A &= \begin{bmatrix} 0 & 0 & 0 & 1 & 0 & 0 \\ 0 & 0 & 0 & 0 & 1 & 0 \\ 0,0548 & 0 & 0 & 0 & 0 & 0 \\ 0 & -1,0319 & 0 & 0 & 0 & 0 \\ 0 & 10,8405 & 0 & 0 & 0 & 0 \end{bmatrix} \\
B &= \begin{bmatrix} 0 & 0 \\ 0 & 0 \\ 0 & 0 \\ 1,46 \cdot 10^{-5} & 1,46 \cdot 10^{-5} \\ -1,4 \cdot 10^{-3} & 1,4 \cdot 10^{-3} \\ 0 & 0 \end{bmatrix} \\
x &= [\xi \quad p \quad \lambda \quad \dot{\xi} \quad \dot{p} \quad \dot{\lambda}]^T
\end{aligned} \tag{4}$$

The B matrix coefficients are very small because the input variable is rotation speed squared, so its range is much larger than the states.

2.3 Hardware Implementations and Limitations

The built system has two encoders and an IMU for angle measurement. The pitch encoder has 0.18 degrees of precision and the travel angle 0.9 degrees, but, other than the quantization, they have no significant noise. Alternatively, the elevation measurement is made by sensor fusion using the FreeIMU library. The actuators have a 8bits precision on its input.

The high quantization on the travel angle and the noise on the elevation angle imposes a limitation on the system performance and causes an oscillation not only on the travel angle but on the elevation angle as well (because of the coupling).

3 Linear Quadratic Regulator

The controller chosen for this paper is the LQR augmented with integrators as in Figure 5 and described in (Fadali and Visioli, 2012). The initial estimation for the Q and R matrices was done with the Bryson rule and empirically adjusted.

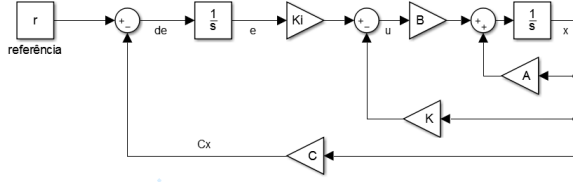


Figure 5: Augmented System Block Diagram

The final LQR gain matrix for the simplified and complete model are , respectively, presented in equations (5) and (6):

$$K_{LQR_s} = \begin{bmatrix} -4.37 \cdot 10^3 & -4.37 \cdot 10^3 \\ 5.48 \cdot 10^3 & -5.48 \cdot 10^3 \\ 3.72 \cdot 10^5 & 3.72 \cdot 10^5 \\ -6.06 \cdot 10^5 & 6.06 \cdot 10^5 \\ -4.29 \cdot 10^5 & 4.29 \cdot 10^5 \\ 1.57 \cdot 10^5 & 1.57 \cdot 10^5 \\ -7.08 \cdot 10^4 & 7.08 \cdot 10^4 \\ -1.65 \cdot 10^5 & 1.65 \cdot 10^5 \end{bmatrix}^T \quad (5)$$

$$K_{LQR_c} = \begin{bmatrix} -4.37 \cdot 10^3 & -4.37 \cdot 10^3 \\ 5.67 \cdot 10^3 & -5.67 \cdot 10^3 \\ 3.75 \cdot 10^5 & 3.75 \cdot 10^5 \\ -5.56 \cdot 10^5 & 5.56 \cdot 10^5 \\ -4.28 \cdot 10^5 & 4.28 \cdot 10^5 \\ 1.57 \cdot 10^5 & 1.57 \cdot 10^5 \\ -7.08 \cdot 10^4 & 7.08 \cdot 10^4 \\ -1.65 \cdot 10^5 & 1.65 \cdot 10^5 \end{bmatrix}^T \quad (6)$$

As both controllers were designed with the same Q and R matrices, they would try to minimize the same cost function.

As expected, both matrices are very alike and are more disparate on the travel and roll angles, and on the travel error integrator.

4 Simulation and Practical Results

To simulate this system, white noise perturbations were considered in all three angles, the pitch and travel angle with variance of 10^{-8} and the elevation angle of 10^{-4} due to the significantly higher noise of the IMU sensor when compared with the encoders. The encoders' quantization were also considered since the travel angle has 0.9 degrees of quantization and it could affect the system. The results are presented in figures 6, 7 and 8.

In Figures 6 and 7 it is presented a comparison between the practical and simulation of the system with the controller designed from the complete linear model.

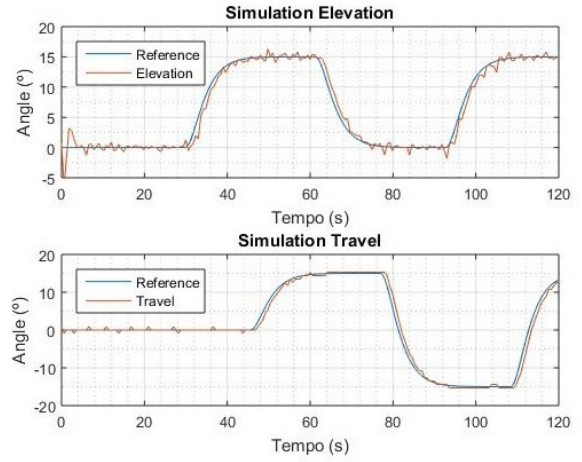


Figure 6: Simulation with the Complete Model design

Furthermore, in Figure 8 it is exposed the practical results of the controller designed with simplified linear model. Comparing figures 7 and 8 it is possible to notice a significant increase in oscillation when the simplified model is used.

The practical results for the control design us-

5 Conclusions

The complete nonlinear model resulted in a good simulator with similar responses to the practical results. Some disparities can be seen and are expected, since there are numerous effects in a practical experiment that were not considered on the simulation — like the effect of the ground over the actuator or air currents. Even so, the results were very similar and it is possible to conclude that the model generated by the Newton-Euler iterative method is good to simulate the real system.

Further on, the good results for the nonlinear model indicate the possibility to develop a model based nonlinear control to this system as a future work. This could be justified by the possibility to increase the operating range of the system and as a comparison between linear and nonlinear control for this system.

The second conclusion is drawn comparing the results of the complete and simplified design. Albeit both resulted in a stable system, the one designed with the simplified model exhibited more oscillations in both the travel and elevation angle.

The oscillation on the travel angle is expected because the linear model assumes that the roll angle is an inertial system when it is, in fact, a pendulum. This means that there is an oscillatory trend on this angle that is neither seen nor compensated by the control. Evidently, the bigger the bias between the rotation axis of the roll angle and its CM, the bigger these oscillations are. Still, it is better to include this dynamics on the control design.

In addition, the increase in the elevation angle comes directly from the coupling between the roll and the elevation angles, since the coupling effect increases with an increase in the oscillations.

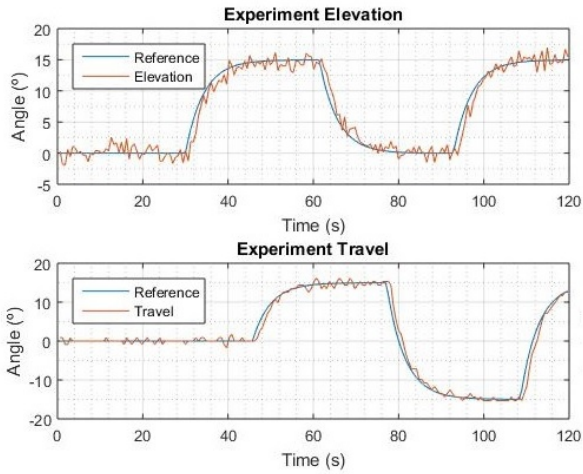


Figure 7: Experiment with the Complete Model design

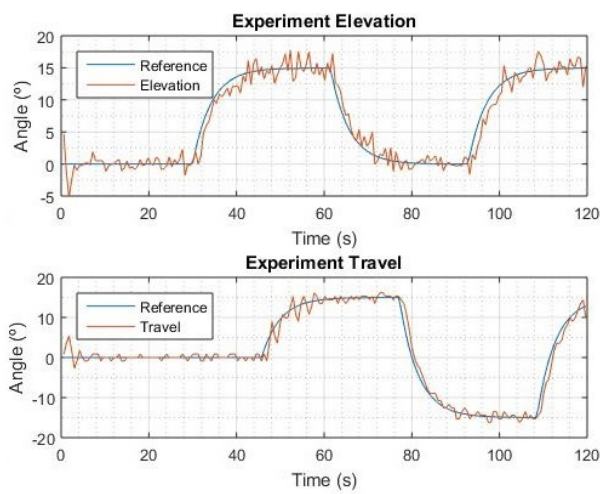


Figure 8: Experiment with the Simplified Model design

ing the full model can be watched on Youtube¹.

¹<https://www.youtube.com/watch?v=IddgHR0qjSQ>

References

- Boby, R. I., Mansor, H., Gunawan, T. S. and Khan, S. (2014). Robust adaptive LQR control of nonlinear system application to 3-DOF flight control system, *Smart Instrumentation, Measurement and Applications (IC-SIMA), 2014 IEEE International Conference on*, IEEE, pp. 1–4.
- Choudhary, S. K. (2014). LQR based PID controller design for 3-DOF helicopter system, *International Journal of Computer, Information, Systems and Control Engineering* **8**(8): 1375–1380.
- Craig, J. J. (2005). *Introduction to robotics: mechanics and control*, Vol. 3, Pearson Prentice Hall Upper Saddle River.
- Fadali, M. S. and Visioli, A. (2012). *Digital control engineering: analysis and design*, Academic Press.
- Liu, H., Lu, G. and Zhong, Y. (2013). Robust LQR attitude control of a 3-DOF laboratory helicopter for aggressive maneuvers, *IEEE Transactions on Industrial Electronics* **60**(10): 4627–4636.
- Liu, H., Xi, J. and Zhong, Y. (2014). Robust hierarchical control of a laboratory helicopter, *Journal of The Franklin Institute* **351**(1): 259–276.
- Pereira, R. L. and Kienitz, K. H. (2014). Robust controllers using generalizations of the LQG/LTR method, *Journal of Control, Automation and Electrical Systems* **25**(3): 273–282.
- Zheng, B. and Zhong, Y. (2011). Robust attitude regulation of a 3-DOF helicopter benchmark: theory and experiments, *IEEE Transactions on Industrial Electronics* **58**(2): 660–670.